HOST-PATHOGEN INTERACTIONS

A Loss-of-Function Screen Reveals Ras- and Raf-Independent MEK-ERK Signaling During *Chlamydia trachomatis* Infection

Rajendra Kumar Gurumurthy,[1]* André P. Mäurer,[1]* Nikolaus Machuy,[1]* Simone Hess,[1]† Klaus P. Pleissner,[2] Johannes Schuchhardt,[3] Thomas Rudel,[1]‡ Thomas F. Meyer[1]§

(Published 16 March 2010; Volume 3 Issue 113 ra21)

Chlamydiae are obligate intracellular bacterial pathogens that have a major effect on human health. Because of their intimate association with their host, chlamydiae depend on various host cell functions for their survival. Here, we present an RNA-interference–based screen in human epithelial cells that identified 59 host factors that either positively or negatively influenced the replication of *Chlamydia trachomatis* (*Ctr*). Two factors, K-Ras and Raf-1, which are members of the canonical Ras–Raf–MEK (mitogen-activated or extracellular signal–regulated protein kinase kinase)–ERK (extracellular signal–regulated kinase) pathway, were identified as central components of signaling networks associated with hits from the screen. Depletion of Ras or Raf in HeLa cells increased pathogen growth. Mechanistic analyses revealed that ERK was activated independently of K-Ras and Raf-1. Infection with *Ctr* led to the Akt-dependent, increased phosphorylation (and inactivation) of Raf-1 at serine-259. Furthermore, phosphorylated Raf-1 relocalized from the cytoplasm to the intracellular bacterial inclusion in an Akt- and 14-3-3β–dependent manner. Together, these findings not only show that *Chlamydia* regulates components of an important host cell signaling pathway, but also provide mechanistic insights into how this is achieved.

INTRODUCTION

Chlamydiae are Gram-negative, obligate, intracellular bacterial pathogens and the causative agents of a wide range of human and animal diseases. *Chlamydia trachomatis* (*Ctr*) is a human pathogen associated with several diseases, including sexually transmitted diseases (*1*) and preventable blindness (trachoma) (*2*). The developmental cycle of *Ctr* alternates between two functionally and morphologically distinct forms: the extracellular, infectious, metabolically inactive elementary body (EB) and the intracellular, metabolically active, replicating reticulate body (RB). EBs infect host cells and differentiate into RBs within a membrane-bound, protective vacuole called the inclusion. RBs multiply, and at the end of the cycle they redifferentiate into EBs, which are released from cells to initiate a new developmental cycle by infecting neighboring cells (*3*).

To ensure successful entry, survival, and propagation, *Chlamydia* interacts with its host cell in several different ways. *Chlamydia* has a type III secretion system, which releases bacterial effector proteins into the host cell (*4*, *5*). The production of these effectors varies with the developmental cycle (*6*). In addition, host cell proteins, including 14-3-3β and Bcl2-associated agonist of cell death (BAD), are recruited to the inclusion, which results in the modulation of host cell processes (*7*). *Chlamydia* targets various functions of the infected cell to acquire amino acids (*8*), nucleotides (*9*), and other precursors from the host. The pathogen is also capable of manipulating host cell pathways and functions, such as proapoptotic defense mechanisms (*10*) and the Ras–Raf–MEK (mitogen-activated or extracellular signal–regulated protein kinase kinase)–ERK (extracellular signal–regulated kinase) cascade (*11*), for its own benefit. ERK and its downstream target cytosolic phospholipase A_2 ($cPLA_2$) are activated during infection with *Chlamydia* (*11*). Although bacterial and host factors contribute to the establishment and success of the infection, the underlying host mechanisms remain widely elusive.

The Ras-Raf-MEK-ERK pathway plays a key role in fundamental physiological functions, such as cell proliferation, cell cycle, survival, and apoptosis (*12*). Raf-1 is activated by a direct interaction with a guanosine triphosphate (GTP)–bound, active molecule of the guanosine triphosphatase (GTPase) Ras, which recruits Raf-1 to the plasma membrane (*13*). At the membrane, kinases, such as p21-activated kinase (PAK) and Src family members, activate Raf-1 by multiple phosphorylation reactions (*14*). The active form of Raf-1 phosphorylates MEK1 and MEK2. The predominant downstream targets of the MEKs are the mitogen-activated protein kinases (MAPKs) ERK1 and ERK2 (*13*). The ERKs phosphorylate multiple transcription factors, including Ets-1, c-Jun, c-Myc, ribosomal S6 kinase (p90RSK), and nuclear factor κB (NF-κB) (*15*, *16*). In addition to following a classical linear cascade, the Ras-Raf-MEK-ERK pathway is also widely branched (*12*).

The silencing of gene expression by RNA interference (RNAi) technology is proving to be a powerful tool to investigate the function of host proteins. High-throughput applications of RNAi have led to insights into events such as cytokinesis (*17*), Wnt signaling (*18*), Janus-activated kinase (JAK)–signal transducer and activator of transcription (STAT) signaling (*19*), and host-pathogen interactions (*20*, *21*). Two relevant loss-of-function screens have revealed a role for the multiprotein Tim-Tom complex in *Chlamydia caviae* infection (*22*) and highlighted the importance of the receptor tyrosine kinase platelet-derived growth factor receptor β (PDGFR-β) and the kinase ABL for the efficient uptake of *Ctr* by host cells (*23*). However, these studies

[1]Department of Molecular Biology, Max Planck Institute for Infection Biology, 10117 Berlin, Germany. [2]Core Facility Bioinformatics, Max Planck Institute for Infection Biology, 10117 Berlin, Germany. [3]MicroDiscovery GmbH, 10405 Berlin, Germany.
*These authors contributed equally to this work.
†Present address: Hannover Medical School, 30625 Hannover, Germany.
‡Present address: Department of Microbiology, Biocenter, University of Würzburg, 97074 Würzburg, Germany.
§To whom correspondence should be addressed. E-mail: meyer@mpiib-berlin.mpg.de

were carried out in *Drosophila* cells, a non-native host cell type for *Chlamydia*, which supports the full developmental cycle of *C. caviae* but not that of *Ctr*.

Here, we present a systematic siRNA-based loss-of-function screen aimed at discovering host cell factors that interfere with the entry, survival, and replication of *Ctr* within human epithelial cells. We identified 59 host cell factors whose knockdown altered *Ctr* infectivity. These factors included K-Ras and Raf-1, which when knocked down led to the increased growth of *Ctr*. Despite the depletion of K-Ras and Raf-1, ERK was still activated after the infection of cells with *Ctr*, which was accompanied by the strong stimulation of $cPLA_2$. This suggested that activation of ERK in *Ctr*-infected cells occurred through a K-Ras– and Raf-1–independent mechanism. Infection by *Ctr* also led to the Akt1- and Akt2-dependent phosphorylation of Raf-1 at Ser^{259}, a modification known to inactivate Raf-1 (*24*, *25*). In addition, we showed that Raf-1 was recruited to the inclusion in an Akt- and 14-3-3β–dependent manner. These data suggest that infection with *Ctr* triggers a modular regulation of components of the Ras-Raf-MEK-ERK pathway to support growth of the pathogen.

RESULTS

A functional RNAi screen for host cell factors critical to *Ctr* infection and development is established

To identify host cell factors that have crucial functions during *Ctr* infection and the progression of the pathogen's developmental cycle (Fig. 1A), we established a two-step assay that enabled us to determine (i) the number of EBs that infected cells and differentiated into RBs inside host cells (termed infection) and (ii) the resulting infectious progeny (termed infectivity). We used fluorescence microscopy as a read-out system (Fig. 1B). One day before transfection with small interfering RNAs (siRNAs),

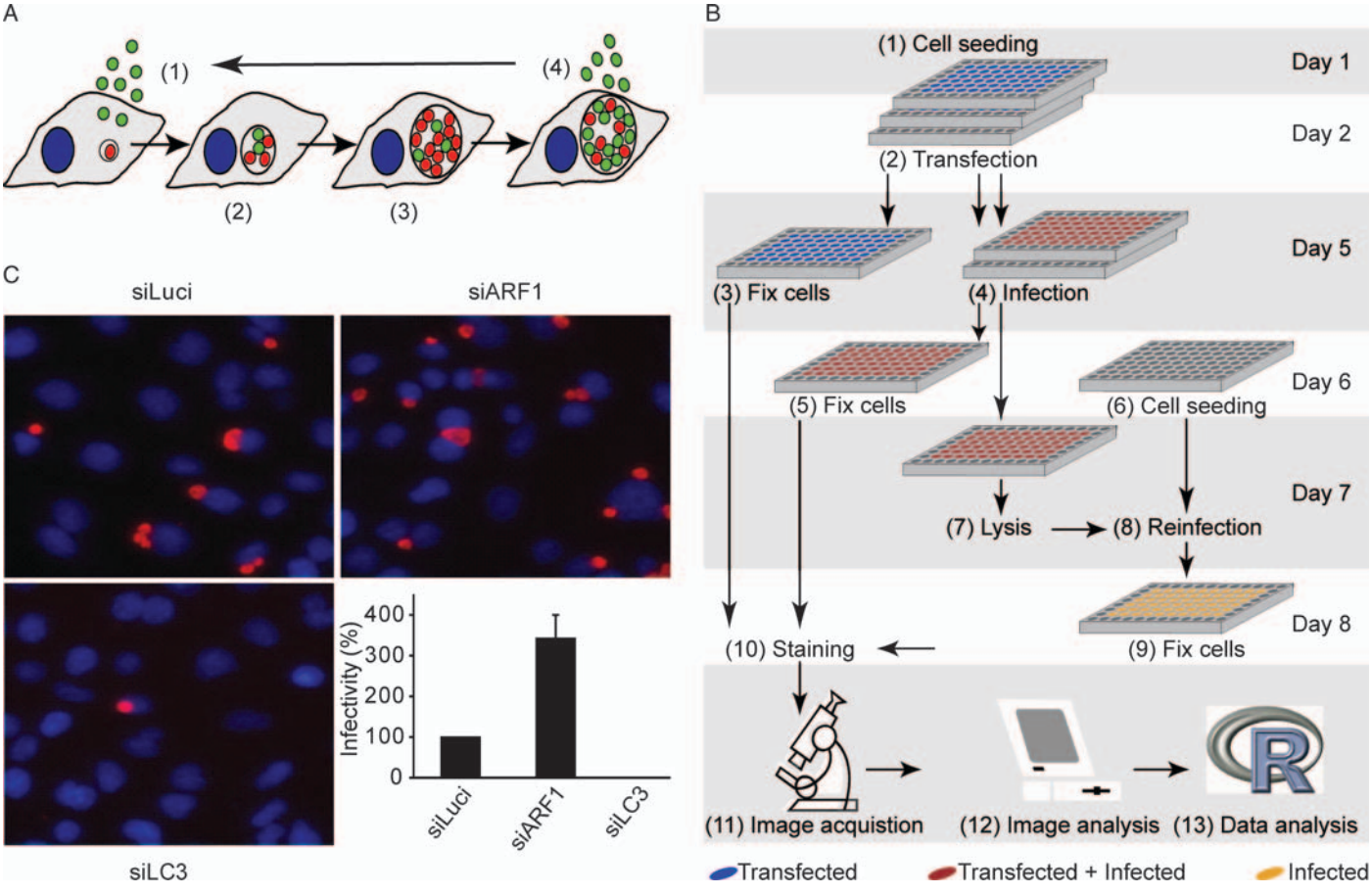

Fig. 1. A loss-of-function screen for host factors involved in the development cycle of *Chlamydia* (*Ctr*). (**A**) The development cycle of *Ctr*. *Ctr* EBs (green) enter the host cell (step 1) and differentiate to RBs (red) (steps 1 and 2). The RBs multiply (step 3) and redifferentiate back to EBs (step 4) that can infect new host cells. (**B**) Cells were seeded (step 1) and transfected (step 2) in triplicate. At 72 hours after transfection, one plate was fixed (step 3) to monitor any specific effects of the siRNAs used on cell growth. The remaining two plates were infected with *Ctr* (step 4), and at 24 hours after infection one plate was fixed to evaluate the number and size of *Ctr* infectious particles (infection, step 5). Fresh cells were seeded (step 6) and infected with the lysate from the second infected plate at 48 hours after infection (steps 7 and 8), fixed 24 hours later to measure infectivity (step 9). Nuclei in the host cells of all of the plates were stained with Hoechst and *Chlamydia* were detected with an antibody against *Ctr* (step 10). Images were acquired (step 11) and subjected to image and data analysis (steps 12 and 13). (**C**) The siRNAs siLuci, siARF1, and siLC3 were established as having no effect, an activating effect, or an inhibitory effect, respectively, on infectivity of *Ctr* from transfected cells. Shown are representative images and the normalized infectivity rates ± SD of three independent experiments. siLuci was used as a reference control.

HeLa cells were seeded in three 96-well plates. The cells in one plate were fixed 72 hours after transfection to evaluate the possible effects of gene knockdown on cell number. At the same time, cells in both of the remaining plates were infected with *Ctr*. Cells in one of the plates were used to monitor the infection rate 24 hours after infection, whereas cells in the other plate were lysed 48 hours after infection, and dilutions of the lysates were used to infect nontransfected HeLa cells, which were fixed 24 hours after infection to monitor the infectivity rate of *Ctr*. All of the plates were then processed for immunofluorescence microscopy by staining the cell nuclei with Hoechst dye, whereas bacterial inclusions were detected with an antibody against the major outer membrane protein (MOMP) of *Ctr*. The number of inclusions per cell and sizes of these inclusions were determined by automated microscopic readout (fig. S1).

To test the reliability of the functional assay, we used siRNAs specific for the small GTPase adenosine diphosphate (ADP) ribosylation factor (ARF1) (siARF1) and a combination of siRNAs specific for the light-chain subunits of the microtubule-associated proteins MAP1LC3A and MAP1LC3B (siLC3). Transfection of cells with siARF1 before infection with *Ctr* resulted in larger inclusions and higher infectivity than occurred in cells transfected with an siRNA against luciferase (siLuci) (thus, siARF1 was considered an activating control), whereas siLC3-mediated knockdown of MAP1LC3A and MAP1LC3B before infection resulted in the formation of smaller inclusions and almost no infectivity (Fig. 1C and fig. S2) (thus, siLC3 was considered an inhibitory control). Three siRNA libraries were screened: a kinase library that targeted 646 kinases and kinase-binding proteins, an apoptosis library directed against 418 apoptosis-related genes, and a custom library that targeted 471 genes with a broad range of cellular functions. Altogether, 1289 unique genes were targeted with two pooled siRNAs per gene. Each pooled siRNA was tested a minimum of three times in 96-well plates. For further analyses, we concentrated on infectivity. Only plates in which the controls showed increased or decreased infectivity rates of at least twofold were analyzed further.

For quality control, a platewise correlation coefficient matrix was generated for each of the tested parameters in the assay, based on all samples (fig. S3). Infectivity data were normalized by B-score and percent-of-control (POC) analyses (Fig. 2A, fig. S4, and table S1), and targeted genes were designated as primary hits according to defined thresholds, as described in Materials and Methods. With this approach, we identified 204 and 203 primary hits from the B-score and POC analyses, respectively. For further analyses, we focused on the 80 genes common to both methods, in addition to 26 genes that were identified exclusively from either the B-score or POC methods, giving a total of 132 primary hits.

Proteins required for *Ctr* infectivity are validated

To validate the initial 132 hits, we performed a second round of screening that used four independent, newly designed siRNAs for each target gene (Fig. 2B). Data were normalized by POC. Validated hits that showed a minimum change in infectivity of twofold with at least three siRNAs were classified as strong, those that exhibited a 1.5-fold effect with at least three siRNAs were classified as medium hits, and those that exhibited a 1.5-fold effect with two siRNAs were categorized as weak hits. Primary hits that did not meet the validation criteria or that showed opposing phenotypes were grouped as "not validated." With these stringent criteria, of the 132 primary hits subjected to hit validation, 30 qualified as weak, 15 as medium, and 14 as strong hits (Fig. 2B, tables S2 and S3, and fig. S5). Of the primary hits that were exclusively derived from the B-score and POC methods, we achieved a validation rate of 35 and 46%, respectively; a validation rate of 48% was achieved by selecting hits common to both methods (Fig. 2C). These validation rates indicate that control-based normalization of RNAi screening data may be more reliable than sample-based normalization.

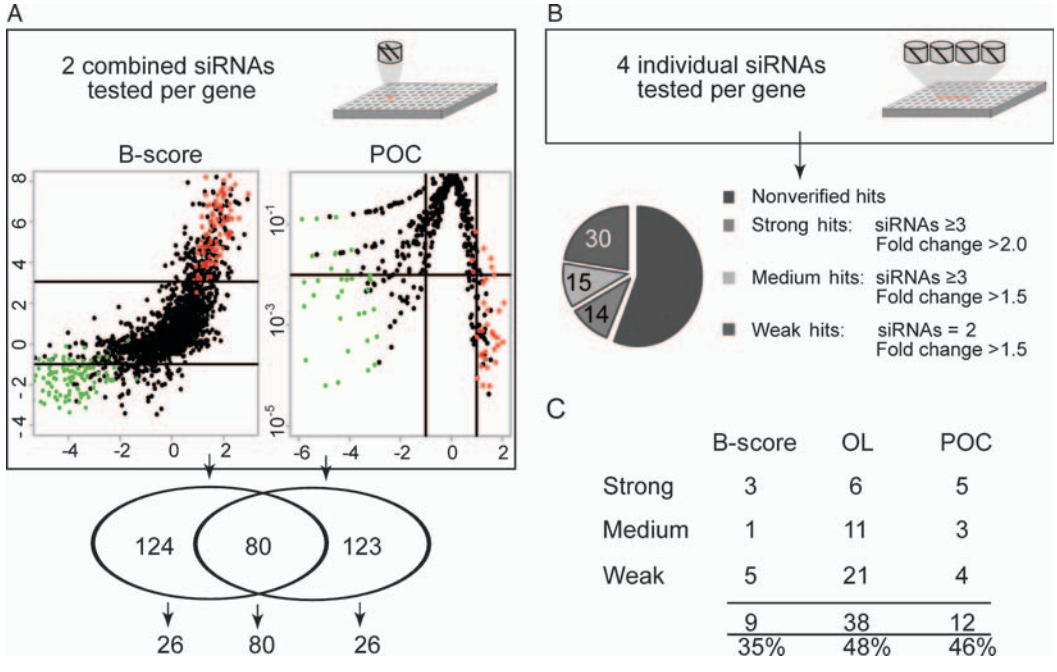

Fig. 2. Identification and validation of hits from the primary screen. (A) Infectivity data of cells transfected with a pool of two siRNAs per gene were analyzed in parallel by two statistical normalization methods: B-score and POC. siLC3 inhibitory controls are marked in green, siARF1 activating controls in red, and samples in black. The black lines indicate the defined thresholds used for defining the primary hits. All of the 80 overlapping primary hits from both statistical analysis methods and the 26 nonoverlapping primary hits that were identified exclusively with the B-score and POC methods were chosen for further validation. (B) Validation of the hits was performed for 132 primary hits with four independent siRNAs per gene. Data were analyzed by POC normalization and validated hits were grouped into "strong," "medium," and "weak" hits according to the number of siRNAs that elicited a biological effect. (C) Validated hits are grouped according to the statistical analysis used for the definition of primary hits. The numbers of scored hits from each of the methods of analysis used in the primary screen, as well as the overlapping genes, are shown.

Network analysis identifies a coherent network of interactions important for *Ctr* infectivity

To identify functional modules and signaling pathways that were potentially associated with the 59 validated hits, we carried out gene ontology (GO) analysis with GOstats software and pathway analysis with Ingenuity Pathway Analysis (IPA) software. First, we looked for enriched GO terms associated with the validated hits according to biological process or molecular function. We found an over-representation of genes associated with small GTPases and especially with Ras-related signal transduction (Fig. 3A).

Next, we performed an in silico network analysis with IPA and categorized the hits according to their proposed molecular and cellular functions. Multiple functional groups were significantly ($P < 0.05$; log < −2) enriched in all three hit categories (Fig. 3B). Two representative functions, cell death and cell morphology, were merged and subjected to an assisted network analysis by IPA (Fig. 3C) on the basis of known protein-protein interactions or roles in activation, inhibition of proteins, and transcription of genes. Several connections were apparent; for example, the proapoptotic protein direct inhibitor of apoptosis (IAP)–binding protein with low isoelectric point (pI) (DIABLO) and the tumor necrosis factor receptor (TNFR) superfamily members lymphotoxin β receptor (LTBR) and TNFR18 are connected to the E3 ubiquitin ligase TNFR-associated factor 2 (TRAF2) through protein-protein interactions (*26*–*28*).The receptor phosphatidylinositol-5-phosphate 4-kinase type 2 beta (PIP5K2B) binds to tumor necrosis factor receptor superfamily member 1A (TNFRSF1A) (*29*), a known activator of TRAF2

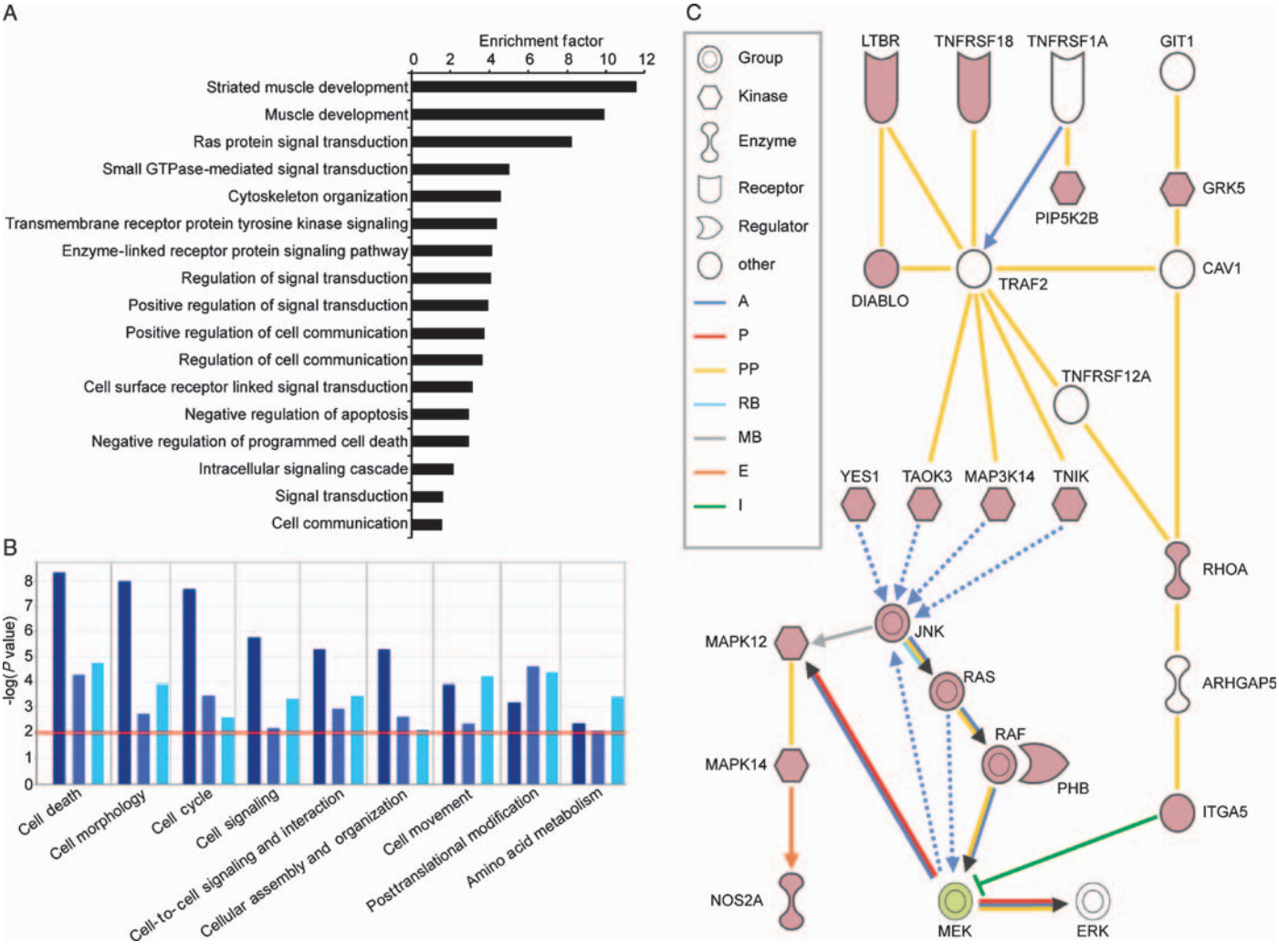

Fig. 3. Gene enrichment and network analysis. (**A**) Statistically significant ($P < 0.05$) enrichment factors of selected biological processes, according to GO, for the 14 hits classified as strong. Enrichment factors and *P* values were calculated with the GOstats R-package in a modification available from the Gaggle Web site (see Materials and Methods). (**B**) The strong, medium, and weak hits (shown as bars from dark blue to light blue) were analyzed with IPA software for prominent functions. Only functions that met the significance threshold (red line) are displayed ($P < 0.01$; log < −2). (**C**) Two representative functions, cell death and cell morphology, were joined and subjected to a curated network analysis. The simplified network based on the interactions predicted by IPA is depicted. Hits are designated in colors based on phenotypes: green for those targets that inhibited infectivity and red for those gene targets that increased infectivity upon knockdown. Other proteins (non-hits) were added to complement the networks (displayed in white). The connections between the proteins are depicted as follows: A, activation; PP, protein-protein interaction; E, expression; RB, regulation of binding; P, phosphorylation; MB, member; I, inhibition. Solid lines show direct interactions, whereas dashed lines show indirect interactions.

(*30*). Additionally, we found that G protein–coupled receptor kinase 5 (GRK5), the GTPase RhoA, and integrin α_5 (ITGA5), which we identified in the screen, are connected to TRAF2 through RhoGTPase activating protein 5 (ARHGAP5), caveolin 1 (CAV1), ARF GTPase-activating protein GIT1 (GIT1), and TNFRSF12A. TRAF2 is also connected to the hits serine and threonine-protein kinase TAO3 (TAOK3), MAPK kinase kinase 14 (MAP3K14), and TRAF2 and NCK-interacting protein kinase (TNIK) (*31*–*33*), all of which are serine and threonine protein kinases and known activators of c-Jun N-terminal kinase (JNK), which in turn interacts with Ras (*34*). Mitogen-activated protein kinase 12 (MAPK12), a member of the JNK family, interacts with MAPK14 (*27*), which results in the increased expression of the gene encoding nitric oxide synthase 2 (NOS2) (*35*). Furthermore, Ras activates Raf, which in turn interacts with prohibitin (*36*). Knockdown of the MEK family member MAPK kinase 6 (MAP2K6), another validated hit, led to decreased *Ctr* infectivity, suggesting an alternative role for Ras, Raf, and MEK during infection.

Knockdown of K-Ras and Raf-1 leads to increased *Ctr* infectivity

The Ras-Raf-MEK-ERK pathway is activated after infection with *Ctr*, which leads to the phosphorylation and activation of $cPLA_2$ by ERK (*11*). Blocking the Ras-Raf-MEK-ERK pathway with chemical inhibitors, for example, the MEK inhibitor U0126, decreases the infectivity of *Ctr* and reduces the extent of phosphorylation of $cPLA_2$ (*11*). In contrast, our screening results showed that knockdown of K-Ras and Raf-1 led to increased *Ctr* infectivity (table S3). Knockdown of the other Raf and Ras family members failed to elicit changes in *Ctr* infectivity (fig. S6, A and B). To further elucidate the mechanism by which the Ras-Raf-MEK-ERK pathway was activated during *Ctr* infection, we compared the cellular outcomes generated by chemical inhibitors with those caused by siRNA-mediated knockdown of gene expression. Western blotting analysis revealed that ERK and $cPLA_2$ were strongly phosphorylated 30 hours after infection, whereas the MEK inhibitor U0126 repressed the phosphorylation of ERK and $cPLA_2$ in response to infection (Fig. 4A). Knockdown of MEK also hampered the phosphorylation of ERK after infection with *Ctr* (Fig. 4B), whereas ERK and $cPLA_2$ were still phosphorylated when K-Ras and Raf-1 were knocked down (Fig. 4C). Consistently, U0126 decreased the infectivity of *Ctr* (Fig. 4D), whereas knockdown of K-Ras and Raf-1 led to increased infectivity (Fig. 4E). These data strongly suggest that the phosphorylation of ERK and the phosphorylation and activation of $cPLA_2$ during *Ctr* infection require MEK but not K-Ras or Raf-1. In addition, both the activation of ERK and the depletion of K-Ras and Raf-1 supported the growth of *Chlamydia* within host cells. Thus, we further investigated the fate of Raf-1 during *Ctr* infection.

Raf-1 is phosphorylated at Ser^{259} after *Ctr* infection

Because knockdown of Raf-1 supported the growth of *Chlamydia*, we investigated whether phosphorylation of Raf-1 was influenced by *Ctr* infection. Previous studies showed that Raf-1 is inactivated when it is phosphorylated at Ser^{259} by Akt (*25*, *37*). Our Western blotting analysis revealed

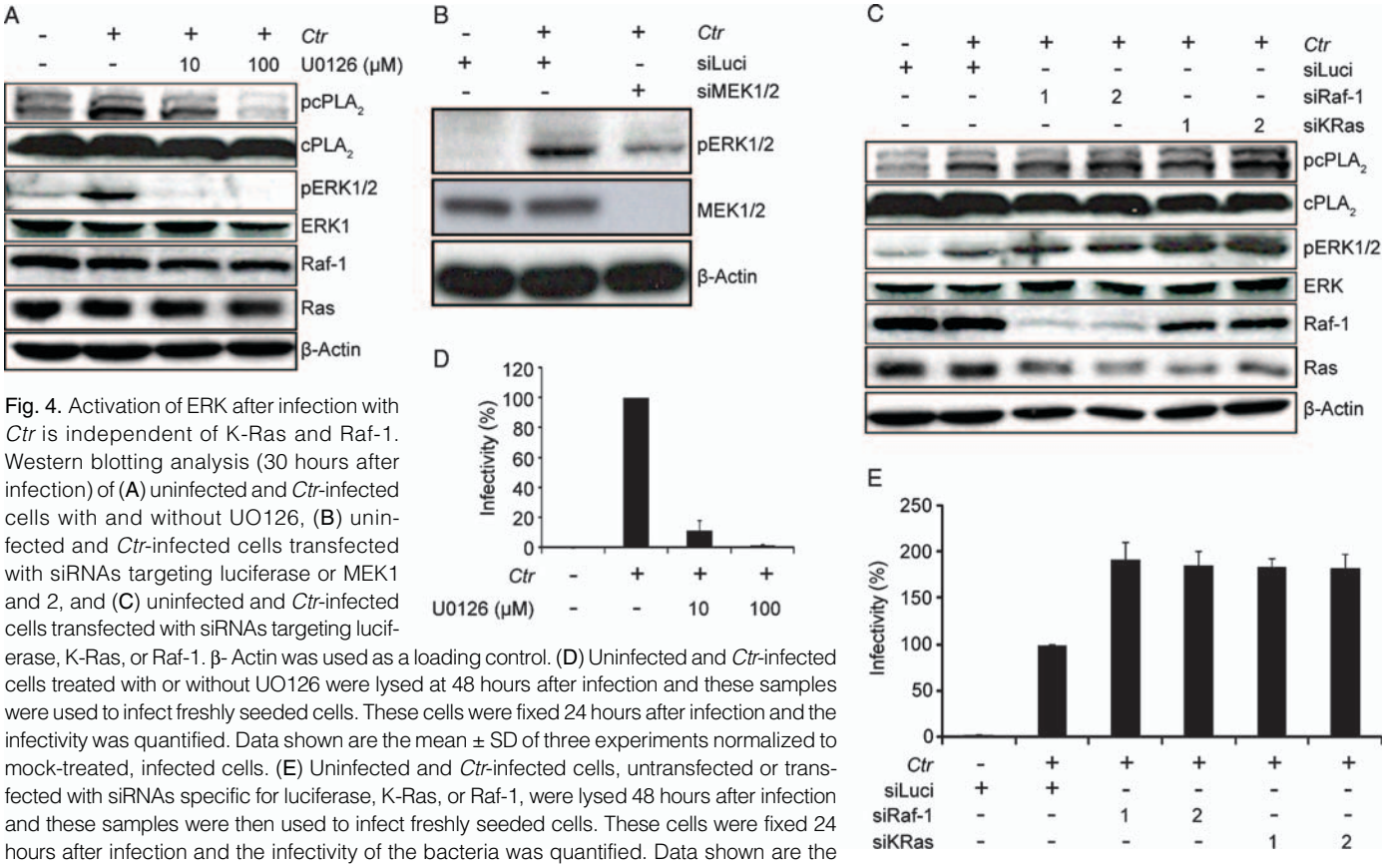

Fig. 4. Activation of ERK after infection with *Ctr* is independent of K-Ras and Raf-1. Western blotting analysis (30 hours after infection) of (**A**) uninfected and *Ctr*-infected cells with and without UO126, (**B**) uninfected and *Ctr*-infected cells transfected with siRNAs targeting luciferase or MEK1 and 2, and (**C**) uninfected and *Ctr*-infected cells transfected with siRNAs targeting luciferase, K-Ras, or Raf-1. β- Actin was used as a loading control. (**D**) Uninfected and *Ctr*-infected cells treated with or without UO126 were lysed at 48 hours after infection and these samples were used to infect freshly seeded cells. These cells were fixed 24 hours after infection and the infectivity was quantified. Data shown are the mean ± SD of three experiments normalized to mock-treated, infected cells. (**E**) Uninfected and *Ctr*-infected cells, untransfected or transfected with siRNAs specific for luciferase, K-Ras, or Raf-1, were lysed 48 hours after infection and these samples were then used to infect freshly seeded cells. These cells were fixed 24 hours after infection and the infectivity of the bacteria was quantified. Data shown are the mean ± SD of three independent experiments normalized to infected and siLuci-transfected cells. Western blots depicted in (A) to (C) are representative of three experiments. For knockdown of K-Ras and Raf-1, two independent siRNAs were used (indicated as 1 and 2).

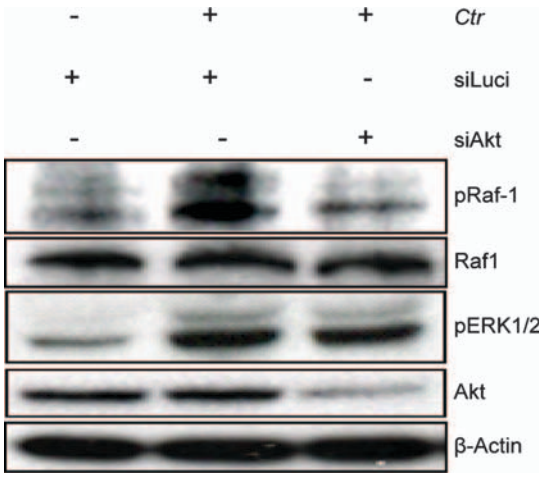

Fig. 5. Phosphorylation of Raf-1 at Ser^{259} after infection with *Ctr* depends on Akt. Uninfected and *Ctr*-infected HeLa cells transfected with siRNAs specific for luciferase or Akt (siAkt1 + 2) were harvested 30 hours after infection and subjected to Western blotting analysis for the detection of Akt, pERK, Raf-1, and pRaf-1 (Ser^{259}). β-Actin was used as a loading control. One blot representative of three independent experiments is shown.

the increased abundance of Raf-1 phosphorylated at Ser^{259} in *Ctr*-infected cells compared to that in uninfected cells, and that knockdown of Akt inhibited this infection-dependent phosphorylation event (Fig. 5). These findings strongly suggested that Raf-1 was inactivated by Akt-dependent phosphorylation at Ser^{259} in response to infection by *Ctr*.

Phosphorylated Raf-1 is recruited to the inclusion in an Akt- and 14-3-3β–dependent manner

During *Ctr* infection, 14-3-3β is recruited to the inclusion by inclusion protein G (IncG) (*38*) and interacts with other host cell proteins, such as BAD (*7*). Phosphorylation of Raf-1 at Ser^{259} results in the binding of Raf-1 to 14-3-3β, a negative regulator of Raf-1 (*25*), and suggests that Raf-1 is redistributed within *Chlamydia*-infected cells (*39*). Thus, we speculated that Raf-1 might also be recruited to the inclusion upon infection in a 14-3-3β– and Akt-dependent manner. Uninfected and *Ctr*-infected HeLa cells were fixed 30 hours after infection and incubated with antibodies against 14-3-3β, Raf-1, or phosphorylated Raf-1 (pRaf-1). Confocal images revealed that Raf-1 and pRaf-1 colocalized with 14-3-3β at the membranes of inclusions in infected cells, whereas in uninfected cells, Raf-1 and pRaf-1 were dispersed throughout the cytoplasm (Fig. 6, A and B). Additionally, ectopic expression of wild-type Raf-1 or a Ser^{259}→Ala mutant of Raf-1 (S259A) revealed that only the wild-type protein localized to the inclusions, whereas the mutant form remained in the cytoplasm of infected cells (Fig. 6, C and D). These data confirmed the phosphorylation-dependent recruitment of Raf-1 to the inclusion.

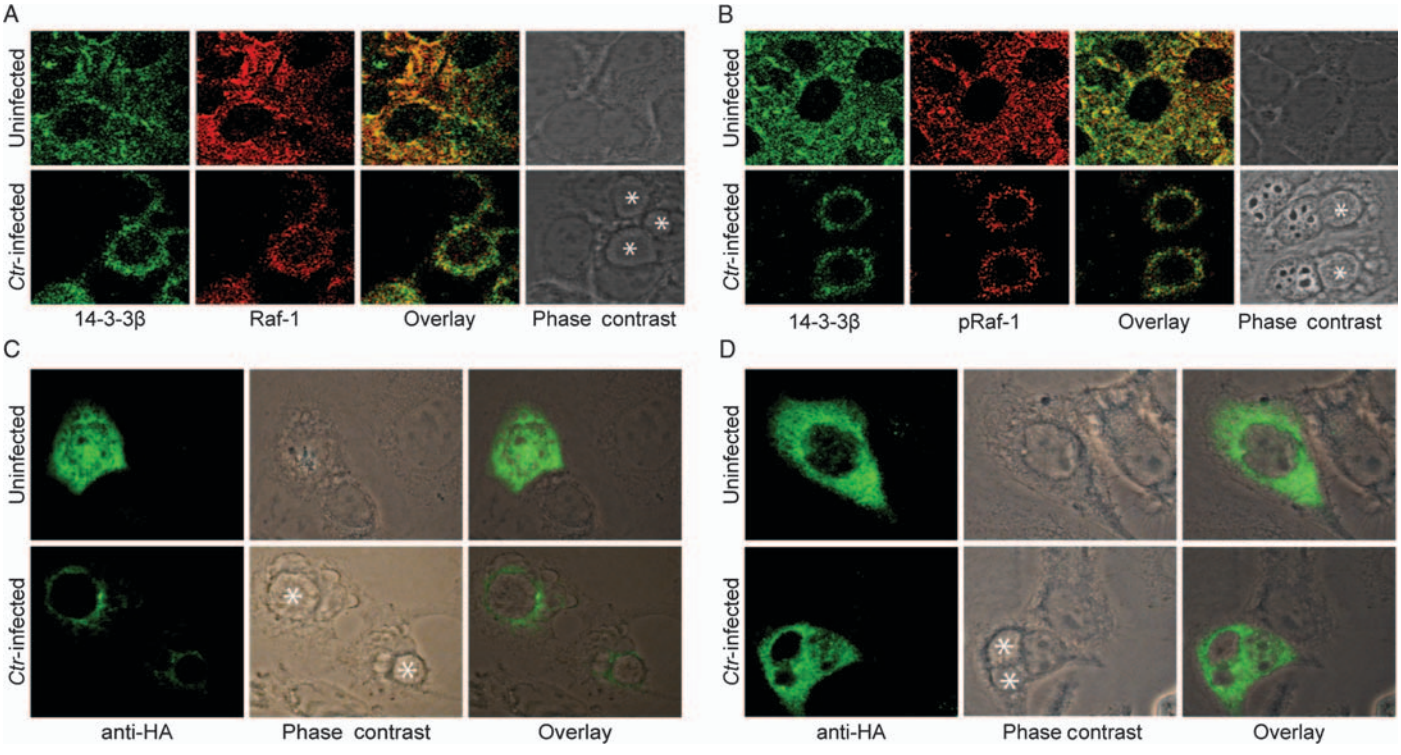

Fig. 6. Translocation of Raf-1 to the *Ctr* inclusion is dependent on its phosphorylation at Ser^{259}. Uninfected and *Ctr*-infected HeLa cells were fixed 30 hours after infection and were incubated with antibodies against 14-3-3β and Raf-1 (**A**) or against 14-3-3β and pRaf-1 at Ser^{259} (**B**). Images were acquired with a confocal microscope. Overlaid images show the colocalization of 14-3-3β and Raf-1 with the *Ctr* inclusion. Uninfected and *Ctr*-infected HeLa cells transfected with plasmids encoding wild-type (WT) Raf-1 (**C**) or the S259A mutant of Raf-1 (**D**) were fixed 30 hours after infection and incubated with an antibody against the HA tag. Images were acquired with a fluorescence microscope. *Ctr* inclusions are marked with an asterisk. Overlaid images show the translocation of WT, but not mutant, Raf-1 to the inclusion. Images are representative of three independent experiments.

To corroborate these observations, we performed fractionation experiments. Uninfected and *Ctr*-infected cells transfected with siRNAs specific for luciferase (a negative control), Akt, or 14-3-3β were separated into subcellular fractions 30 hours after infection, and subjected to Western blotting analysis to detect Raf-1 and, as a marker for *Chlamydia*, the chlamydial heat shock protein 60 kD (Hsp60). As expected, chlamydial Hsp60 was found mainly in the membrane- and organelle-containing fraction of infected cells (Fig. 7, A to C). Consistent with our confocal results, Raf-1 was distributed between the cytosolic and the membrane- and organelle-containing fractions in uninfected control cells transfected with an siRNA against luciferase. In contrast, Raf-1 was predominantly localized to the membrane- and organelle-containing fraction in infected cells (Fig. 7A). However, in Akt-knockdown cells, we observed a lack of redistribution of Raf-1 from the cytosolic fraction to the membrane of both uninfected and *Ctr*-infected cells (Fig. 7B). A similar scenario was observed when cells were depleted of 14-3-3β (Fig. 7C). To investigate whether Raf-1 directly interacted with 14-3-3β at the inclusion, we performed an in situ proximity ligation assay, which enabled us to visualize protein-protein interactions. In *Ctr*-infected cells, we observed a strong accumulation of signals at the inclusion (Fig. 7D). Thus, our findings demonstrate pRaf-1 was recruited to the inclusion in a manner that was dependent on Akt and a direct interaction with 14-3-3β.

DISCUSSION

Here, we present an siRNA-based, loss-of-function screen in human epithelial cells that identified 59 targets that positively or negatively regulated *Ctr* infectivity. Network and gene-enrichment analyses pointed toward K-Ras and Raf-1 as central players involved in signaling networks engaged during *Ctr* infection. To validate this observation, we dissected the functions of K-Ras and Raf-1 during infection. We found that ERK was activated even when Raf-1 was depleted; that Raf-1 was phosphorylated at Ser^{259}, a known inactivating modification of Raf-1, in an Akt-dependent manner; and that phosphorylated Raf-1 was recruited to the inclusion, in a manner that was dependent on Akt and a direct interaction with 14-3-3β. These findings have revealed an unexpected Ras- and Raf-independent MEK-ERK signaling pathway during *Ctr* infection.

We established a screening strategy to identify host factors that influenced *Ctr* infection by measuring infectious progeny (infectivity). This screen uncovered numerous targets with as yet unknown connections to the development of *Chlamydia*. To delineate the relevance of the connections between the identified hits and infection by *Chlamydia*, we generated a curated "interaction network" on the basis of known interactions. In support of this approach, we identified multiple factors that had previously been implicated in *Chlamydia* infection. One of these, TNFRSF1A, which we predicted to be part of the network, is less abundant on the surface of *Ctr*-infected cells than it is on the surface of uninfected cells (*40*). Likewise, we observed increased infectivity by *Ctr* upon knockdown of another TNFR superfamily member, TNFRSF18. Consistent with the inhibitory effect of TNFRSF18 on *Ctr* infectivity, neutralization of its agonist TNF-α increases the infectivity of *C. pneumoniae* (*41*). In addition, the pro-apoptotic protein DIABLO, whose knockdown increased the infectivity of *Ctr*, reportedly interacts with cytosolic inhibitor of apoptosis 1 (cIAP1) and cIAP2 (*42*, *43*), which both constitute essential factors in *Ctr*-induced antiapoptotic mechanisms (*44*). Furthermore, TNFRSF18 and NOS2 were identified as hits in an RNAi-based screen of *Ctr* infection in *Drosophila* cells (*23*). Together, our analysis reveals a coherent

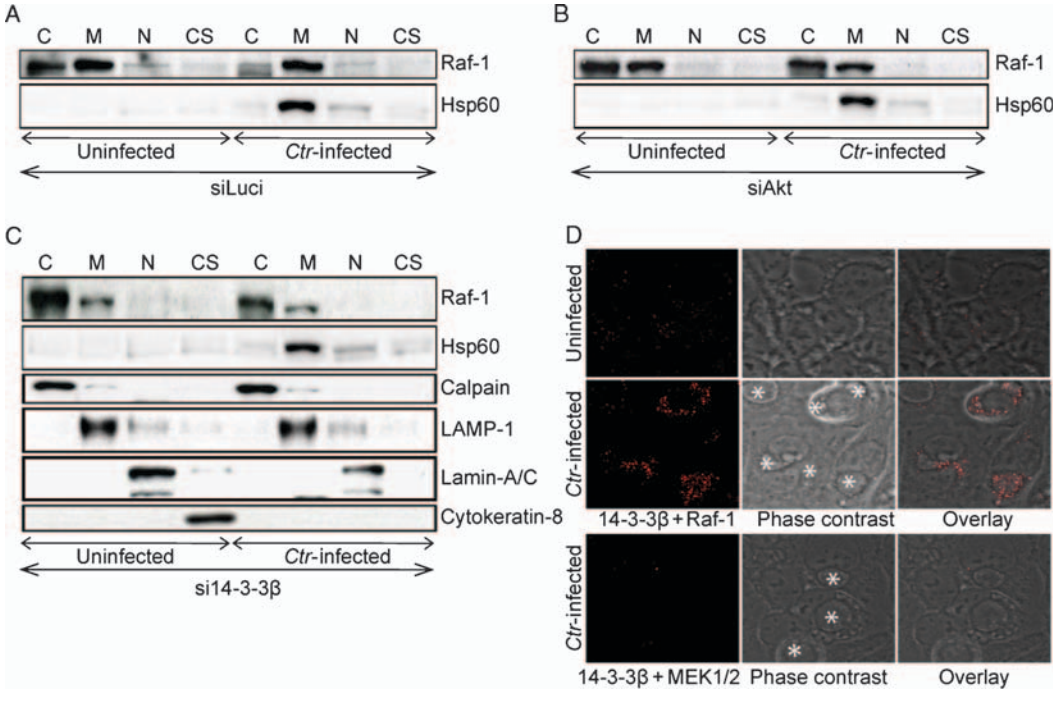

Fig. 7. Translocation of Raf-1 to the inclusion is dependent on Akt and on a direct interaction with 14-3-3β. (**A** to **C**) Uninfected and *Ctr*-infected HeLa cells transfected with siRNAs specific for luciferase (A), Akt1/2 (B), or 14-3-3β (C) were separated into subcellular fractions 30 hours after infection, and subjected to Western blotting analysis for the presence of Raf-1 and chlamydial Hsp60. Calpain, LAMP-1, Lamin-A/C, and cytokeratin-8 were used as markers for cytosolic (C), membrane-organelle (M), nuclear (N), and cytoskeletal (CS) subcellular fractions, respectively. Blots shown are representative of three independent experiments. (**D**) Uninfected and *Ctr*-infected HeLa cells were stained with the Duolink in situ PLA kit with antibodies against Raf-1 and 14-3-3β. Fluorescent dots represent interactions between Raf-1 and 14-3-3β. Antibodies against MEK1/2 and 14-3-3β were used as negative controls. Inclusions are marked with an asterisk. Images shown are representative of three independent experiments.

network of interactions from receptors to signaling effectors, which could modulate an array of transcription factors that play substantial roles in *Ctr* infection.

Ras, Raf, and MEK were placed as central signaling components within the described interaction network. Previous work established that the Ras-Raf-MEK-ERK pathway is activated after infection with *Ctr* and that ERK-mediated activation of $cPLA_2$ is involved in the recruitment of glycerophospholipids to the inclusion (*11*). The Ras-Raf-MEK-ERK signaling module is usually perceived as a linear pathway, with ERK being the effector. However, other studies have unveiled a role for these kinases outside of this established signaling cascade, suggesting the existence of ERK-independent functions of Raf-1 (*45*). Inhibiting the activation of MEK with U0126 results in the abrogation of ERK phosphorylation and prevents the acquisition of glycerophospholipids in *Ctr*-infected cells (*11*). Consistently, we found that treatment of *Ctr*-infected cells with U0126 inhibited the phosphorylation of ERK and decreased the infectivity of *Ctr*. RNAi-mediated silencing of MEK also led to decreased phosphorylation of ERK after infection, suggesting that MEK was required for the activation of ERK and its downstream effectors during *Ctr* infection. In the context of *Ctr* infection, the depletion of K-Ras and Raf-1 did not lead to decreased amounts of phosphorylated ERK and $cPLA_2$, but rather caused an increase in *Ctr* infectivity. Our data suggest that both Ras and Raf-1 are not involved in the downstream activation of MEK and ERK during *Ctr* infection. In agreement with our observations, nonlinear activation of ERK independent of the Ras-Raf-MEK pathway occurs during infection with *Mycobacterium leprae* (*46*). Together, these findings strengthen the critical role of MEK and ERK in the survival of *Ctr* in infected cells and reveal that K-Ras and Raf-1 have antagonistic functions relative to those of MEK and ERK.

The kinase activity of Raf-1 is regulated by the Akt-dependent phosphorylation of a conserved serine residue (Ser^{259}) in its N-terminal regulatory domain (*25*), which inactivates Raf-1 (*14*). Here, we observed the Akt-dependent phosphorylation of Raf-1 at Ser^{259} in *Ctr*-infected cells, which suggested infection-dependent inactivation of Raf-1. Relocation of Raf-1 from the cytoplasm to the inclusion, similar to the recruitment of 14-3-3β (*38*), was dependent on the phosphorylation at Ser^{259}. Furthermore, this relocation event was also dependent on Akt and on a direct interaction between Raf-1 and 14-3-3β. These findings suggest that *Chlamydia* suppresses the function of Raf-1 by sequestering it to the inclusion; activation of Raf-1 normally occurs at the plasma membrane. Consistent with this notion, our screening data showed that depletion of Raf-1 was beneficial for the survival of *Ctr*, indicating that inactivation of Raf-1 by phosphorylation at Ser^{259} and its sequestration to the inclusion act in concert. The host cell protein BAD is also recruited to the inclusion through an interaction with 14-3-3β in a phosphorylation- and Akt-dependent manner; furthermore, siRNA-mediated depletion of Akt reversed this phenotype and sensitized *Ctr*-infected cells to apoptosis (*7*). This implies that 14-3-3β acts as bait, sequestering several host proteins to the inclusion and thereby supporting survival of the pathogen.

In conclusion, this is the first comprehensive, human cell–based, RNAi loss-of-function screen for host cell factors that either positively or negatively affect the developmental cycle of *Ctr*. Detailed investigation of two of these factors, Ras and Raf-1, demonstrated an uncoupled regulation of components of the canonical Ras-Raf-MEK-ERK signaling cascade by *Chlamydia*. Our study also provides evidence for the inactivation of Raf-1 during *Ctr* infection. The functional importance of this inactivation is currently under investigation; however, we hypothesize that *Ctr* specifically inactivates and sequesters Raf-1 to actively interfere with the downstream signaling events induced by Raf-1 independently of MEK and ERK. Our observations indicate that *Ctr* has evolved efficient strategies to uncouple individual modules from otherwise coherent signaling cascades and further advance our understanding of *Chlamydia*–host cell interactions.

MATERIALS AND METHODS

Cell lines and bacterial strains

HeLa cells [American Type Culture Collection (ATCC) CCL-2] were grown in Hepes-buffered growth medium [RPMI (GibCo) supplemented with 10% fetal calf serum (FCS) (Biochrome), 2 mM glutamine, and 1 mM sodium pyruvate], at 37°C in a humidified incubator containing 5% CO_2. *Ctr* serovar L2 (ATCC VR-902B) was propagated in HeLa cells in infection medium (RPMI medium supplemented with 5% FCS).

Propagation of *Chlamydia* and infections

Ctr was propagated in HeLa cells grown in 150-cm^2 cell culture flasks in 24 ml of infection medium. The cells were detached 48 hours after infection with 3-mm glass beads and were centrifuged at 500*g* for 10 min at 4°C. The pelleted cells were resuspended in sucrose-phosphate-glutamate (SPG) buffer and ruptured by vortexing with glass beads. Cell lysates were then centrifuged as before to sediment nuclei and cell debris. The supernatant was further centrifuged at 20,000*g* for 40 min at 4°C, and the resulting bacterial pellet was resuspended in 15 ml of SPG buffer with a 21- to 22-gauge injection needle. Suspensions of *Chlamydia* were stored in aliquots at −75°C until required. HeLa cells were infected with *Ctr* at a multiplicity of infection (MOI) of 0.5 to 3 in infection medium. The medium was refreshed 2 hours after infection, and the cells were grown at 35°C in 5% CO_2 until they were fixed or lysed to be used for reinfections.

Transfection of cells with siRNAs

All siRNAs were purchased from Qiagen. The siRNAs of the custom library were validated at the Max Planck Institute for Infection Biology, for their ability to knockdown messenger RNA (mRNA) expression of target genes by more than 70% compared to control cells transfected with siRNA specific for luciferase, as described previously (*47*). Transfection of cells in 96-well plates with siRNAs was performed with the BioRobot 8000 system (Qiagen). One day before transfection, 1.5×10^3 HeLa cells were seeded in each well of a 96-well plate. For each well, 5 μl of the siRNA stock solution (0.2 μM) was resuspended in 15 μl of RPMI without serum and incubated at room temperature for 10 min, to which 10 μl of a 1:20 diluted solution of Hiperfect (Qiagen) was added, and the mixture was incubated at room temperature for a further 10 min before 25 μl of growth medium was added. Fifty microliters of this transfection mixture was added to each well of the plate in addition to 50 μl of growth medium, which resulted in a final concentration of siRNA of 10 nM. Cells were incubated at 37°C and 5% CO_2 for 72 hours. For the analysis of functional experiments by Western blotting, 1×10^5 cells were seeded into each well of a 12-well plate 24 hours before transfection. Cells were then transfected with Hiperfect transfection reagent according to the manufacturer's guidelines. In brief, 150 ng of specific siRNA was added to RPMI without serum and incubated with 6 μl of Hiperfect in a total volume of 100 μl. After 10 to 15 min, the liposome-siRNA mixture was added to the cells with 1 ml of cell culture medium, which gave a final concentration of siRNA of 10 nM. After 1 day, cells were trypsinized and seeded into new cell culture plates, depending on the experiments. Three days after transfection, the cells were infected and incubated as indicated above.

Infectivity assays

In 96-well plates, HeLa cells were infected as described above. At 2 days after infection, with a BioRobot 8000 system, cells were lysed by adding

NP-40 (Fluka) at a final concentration of 0.06% for 15 min at room temperature. HeLa cells in six-well plates were infected with *Ctr* for 48 hours and then were scraped off the plates with a rubber policeman. The cells were collected in 15-ml tubes containing sterile glass beads and lysed by vortexing (at 2500 rpm for 3 min). For both plate formats, lysates were then diluted 1:100 in infection medium before being transferred to fresh, untreated HeLa cells. After incubation at 35°C and 5% CO_2 for 24 hours, the cells were fixed in ice-cold methanol overnight at 4°C and then processed with the indirect immunofluorescence protocol described below.

Antibodies

Antibodies were obtained from the following sources: Rabbit antibodies against Raf-1, Ras, phosphorylated $cPLA_2$, total $cPLA_2$, total p44 MAPK (ERK1), phosphorylated Raf-1 at Ser^{259}, LAMP-1, MEK1 and MEK2, Akt, and calpain and mouse antibodies against phosphorylated p44 and p42 MAPK (ERK1 and ERK2) were purchased from Cell Signaling Technology. Goat and mouse antibodies against 14-3-3β and rabbit antibodies against Raf-1 (H-71), cytokeratin-8, and the hemagglutinin (HA) epitope (Y-11) were purchased from Santa Cruz Biotechnology. Mouse antibody against lamin-A/C was obtained from Chemicon, mouse antibody against *Chlamydia* Hsp60 was purchased from Alexa, mouse antibody against β-actin was from Sigma, and mouse antibody against *Chlamydia* MOMP KK12 was from the University of Washington. Secondary antibodies conjugated to horseradish peroxidase (HRP) were purchased from Amersham Biosciences and secondary antibodies labeled with the fluorochromes Cy2, Cy3, and Cy5 were from Jackson Immuno Research Laboratories.

Indirect immunofluorescence labeling

Fixed cells (in 96- and 6-well plates) were washed twice with phosphate-buffered saline (PBS) and blocked by incubating with 0.2% bovine serum albumin (BSA) in PBS (blocking buffer) for 30 min at room temperature. Primary mouse antibody against *C. trachomatis* MOMP KK12 (at a 1:10,000 dilution) was added to the cells for 1 hour at room temperature before washing twice with PBS. The Cy3-labeled goat antibody against mouse immunoglobulin G (IgG) was then added at a 1:100 dilution for 1 hour. Host cell nuclei were stained with Hoechst 33342 (Sigma) at a 1:2000 dilution.

Double labeling of Raf-1 or pRaf-1 and 14-3-3β and confocal microscopy

Infected cells were grown on coverslips, washed twice with PBS, and then fixed with ice-cold methanol overnight at 4°C. Cells were again washed twice with PBS and then incubated in blocking buffer as described earlier. The cells were then incubated for 1 hour at room temperature with antibody against 14 3-3β together with antibody against Raf-1 or pRaf-1 (Ser^{259}) in 100 μl of blocking buffer. The cells were then incubated for 1 hour at room temperature with the appropriate fluorochrome-conjugated secondary antibodies at a 1:100 dilution. Between incubation steps, cells were washed three times with PBS. Coverslips were washed and mounted on glass microscopic slides with Moviol. The fluorochromes were visualized with Cy2 and Cy5 filters. A series of images with Z stacks were acquired with a laser scanning confocal microscope (Leica) and analyzed with Imaris Software (Bitplane) and further processed with Photoshop CS3 (Adobe Systems).

Treatment of cells with U0126

Cells (1×10^5) were seeded in each well of a 12-well plate 1 day before infection. Two hours after infection with *Ctr* (at an MOI of 3), 1 ml of fresh infection medium containing either 10 or 100 μM U0126 was added to the cells. Depending on the experiment, cells were harvested for Western blotting analysis or for determination of infectivity.

Automated microscopy and image analysis

The numbers and sizes of chlamydial inclusions and host cells were analyzed with an automated microscope (Olympus Soft Imaging Solutions). Images were taken with DAPI (4′,6-diamidino-2-phenylindole) and Cy3 filter sets (AHF-Analysetechnik) at the same position. ScanR Analysis Software (Olympus Soft Imaging Solutions) was used to automatically identify and quantify inclusions and cells.

Subcellular fractionations

Subcellular fractionation was carried out with the ProteoExtract Subcellular Proteome Extraction kit (Calbiochem) according to the manufacturer's instructions.

Transfections with pcDNA3

HeLa cells were grown on coverslips in 12-well plates, transfected with 1 μg of plasmid DNA encoding HA-tagged wild-type Raf-1 (pcDNA3-Raf-1-WT) or the HA-tagged S259A mutant of Raf-1 (pcDNA3-Raf-1-S259A) with Lipofectamine 2000 (Invitrogen), as described by the manufacturer. Twenty-four hours later, cells were infected with *Ctr* at an MOI of 2. Thirty hours after infection, cells were washed twice with PBS and fixed with ice-cold methanol overnight at 4°C. Cells were again washed twice with PBS and then incubated with blocking buffer as described earlier. The cells were then incubated with primary antibody against the HA tag for 1 hour at room temperature. Cells were then incubated with the secondary fluorochrome-conjugated antibody at a 1:100 dilution for 1 hour at room temperature. Between incubation steps, cells were washed three times with PBS. Coverslips were washed and mounted on glass microscopic slides with Moviol. Images were acquired with a fluorescent microscope (Leica) and processed with Photoshop CS3 (Adobe Systems).

Proximity ligation assay

HeLa cells grown on coverslips in 12-well plates were infected with *Ctr*. At 30 hours after infection, cells were washed twice with PBS and then fixed with ice-cold methanol overnight at 4°C. Incubation with antibodies against Raf-1 (H-71), MEK1/2, or 14-3-3β (A-6) was performed with the Proximity Ligation Assay kit (OLINK) according to the manufacturer's instructions. A series of images with Z stacks were acquired with a laser scanning confocal microscope (Leica), analyzed with Imaris Software (Bitplane), and further processed by Photoshop CS3 (Adobe Systems).

SDS-PAGE and Western blotting

Depending on the experiment, untransfected or transfected HeLa cells were grown in six-well plates, infected with *Ctr* as described earlier, and then washed with PBS. To each well 200 μl of 1× SDS sample buffer (3% 2-mercaptoenthanol, 20% glycerin, 0.05% bromphenol blue, 3% SDS) was added. Cell lysates were collected and boiled for 10 min. Samples were stored at −20°C until required. Proteins from the cell lysates were resolved by SDS–polyacrylamide gel electrophoresis (SDS-PAGE), transferred to polyvinylidene difluoride (PVDF) membranes (PerkinElmer Life Sciences), and blocked with 3% milk powder in tris-buffered saline (containing 0.5% Tween 20) for 30 min before incubation with the appropriate antibodies. The bound primary antibodies were incubated with the corresponding HRP-conjugated secondary antibodies. Immunoreactive proteins were detected on an x-ray film directly or with the AIDA Image Analyzer after addition of ECL reagent (Amersham Biosciences).

Statistical analysis

Screening data were corrected for plate-to-plate variability by normalizing compound measurements relative to controls with POC and B-score analyses (*48*). The resulting data from both methods were used for further analysis and

hit classification. For the POC method, P values and $\log_2$ ratios were calculated for each of the samples. Hits were then classified by defining P value (<0.05) and fold change (>2) for the primary screen, and fold change (>1.5) for the hit validation. In the B-score method, hits were scored by transforming the normalized measurements into Z scores. Hits were then classified by defining thresholds of the Z score for both up-regulating and down-regulating phenotypes (3 and −1, respectively).

Gene enrichment and network analysis

For gene enrichment analysis, we modified the R-script available from the Gaggle Web site (http://gaggle.systemsbiology.net/svn/gaggle/PIPE2.0/trunk/PIPEletResourceDir/GOTableEnrichment/GOEnrichmentScript.R). This script applies the R-package GOstats developed by Falcon and Gentleman (*49*) and is available at Bioconductor (http://www.bioconductor.org). Briefly, we defined a gene universe consisting of 1289 genes targeted in our screen and processed different gene hit lists (strong, medium, and weak) against this universe with respect to molecular function (MF), cellular component (CC), and biological process (BP). For the significantly enriched GO terms, we calculated the enrichment factors. Network analysis was carried out with IPA software (http://www.ingenuity.com/).

SUPPLEMENTARY MATERIALS

www.sciencesignaling.org/cgi/content/full/3/113/ra21/DC1
Fig. S1. Overview of the image analysis with Scan R analysis software.
Fig. S2. siRNA controls and plate layout.
Fig. S3. Correlation plot for platewise quality control.
Fig. S4. Two-step normalization for POC analysis.
Fig. S5. Images for validated hits.
Fig. S6. Infectivity phenotypes upon knockdown of Ras and Raf family members.
Descriptions of supplementary tables.
Table S1. Primary screen data list.
Table S2. Hit validation data list.
Table S3. Final hit list.
Table S4. Sequences of siRNAs used in the primary screen.
Table S5. Sequences of the siRNAs used to validate the hits.

REFERENCES AND NOTES

1. R. C. Brunham, J. Rey-Ladino, Immunology of *Chlamydia* infection: Implications for a *Chlamydia trachomatis* vaccine. *Nat. Rev. Immunol.* **5**, 149–161 (2005).
2. H. R. Wright, A. Turner, H. R. Taylor, Trachoma. *Lancet* **371**, 1945–1954 (2008).
3. J. W. Moulder, Interaction of chlamydiae and host cells in vitro. *Microbiol. Rev.* **55**, 143–190 (1991).
4. D. S. Beeckman, T. Geens, J. P. Timmermans, P. Van Oostveldt, D. C. Vanrompay, Identification and characterization of a type III secretion system in *Chlamydophila psittaci*. *Vet. Res.* **39**, 27 (2008).
5. K. A. Fields, D. J. Mead, C. A. Dooley, T. Hackstadt, *Chlamydia trachomatis* type III secretion: Evidence for a functional apparatus during early-cycle development. *Mol. Microbiol.* **48**, 671–683 (2003).
6. A. P. Mäurer, A. Mehlitz, H. J. Mollenkopf, T. F. Meyer, Gene expression profiles of *Chlamydophila pneumoniae* during the developmental cycle and iron depletion-mediated persistence. *PLoS Pathog.* **3**, e83 (2007).
7. P. Verbeke, L. Welter-Stahl, S. Ying, J. Hansen, G. Hacker, T. Darville, D. M. Ojcius, Recruitment of BAD by the *Chlamydia trachomatis* vacuole correlates with host-cell survival. *PLoS Pathog.* **2**, e45 (2006).
8. J. Gussmann, H. M. Al-Younes, P. R. Braun, V. Brinkmann, T. F. Meyer, Long-term effects of natural amino acids on infection with *Chlamydia trachomatis*. *Microb. Pathog.* **44**, 438–447 (2008).
9. G. McClarty, B. Qin, Pyrimidine metabolism by intracellular *Chlamydia psittaci*. *J. Bacteriol.* **175**, 4652–4661 (1993).
10. T. Fan, H. Lu, H. Hu, L. Shi, G. A. McClarty, D. M. Nance, A. H. Greenberg, G. Zhong, Inhibition of apoptosis in chlamydia-infected cells: Blockade of mitochondrial cytochrome c release and caspase activation. *J. Exp. Med.* **187**, 487–496 (1998).
11. H. Su, G. McClarty, F. Dong, G. M. Hatch, Z. K. Pan, G. Zhong, Activation of Raf/MEK/ERK/cPLA2 signaling pathway is essential for chlamydial acquisition of host glycerophospholipids. *J. Biol. Chem.* **279**, 9409–9416 (2004).
12. W. Kolch, Meaningful relationships: The regulation of the Ras/Raf/MEK/ERK pathway by protein interactions. *Biochem. J.* **351** (Pt 2), 289–305 (2000).
13. J. A. McCubrey, L. S. Steelman, W. H. Chappell, S. L. Abrams, E. W. Wong, F. Chang, B. Lehmann, D. M. Terrian, M. Milella, A. Tafuri, F. Stivala, M. Libra, J. Basecke, C. Evangelisti, A. M. Martelli, R. A. Franklin, Roles of the Raf/MEK/ERK pathway in cell growth, malignant transformation and drug resistance. *Biochim. Biophys. Acta* **1773**, 1263–1284 (2007).
14. D. K. Morrison, R. E. Cutler, The complexity of Raf-1 regulation. *Curr. Opin. Cell Biol.* **9**, 174–179 (1997).
15. F. Chang, L. S. Steelman, J. T. Lee, J. G. Shelton, P. M. Navolanic, W. L. Blalock, R. A. Franklin, J. A. McCubrey, Signal transduction mediated by the Ras/Raf/MEK/ERK pathway from cytokine receptors to transcription factors: Potential targeting for therapeutic intervention. *Leukemia* **17**, 1263–1293 (2003).
16. H. Nakano, M. Shindo, S. Sakon, S. Nishinaka, M. Mihara, H. Yagita, K. Okumura, Differential regulation of IκB kinase α and β by two upstream kinases, NF-κB-inducing kinase and mitogen-activated protein kinase/ERK kinase kinase-1. *Proc. Natl. Acad. Sci. U.S.A.* **95**, 3537–3542 (1998).
17. U. S. Eggert, A. A. Kiger, C. Richter, Z. E. Perlman, N. Perrimon, T. J. Mitchison, C. M. Field, Parallel chemical genetic and genome-wide RNAi screens identify cytokinesis inhibitors and targets. *PLoS Biol.* **2**, e379 (2004).
18. R. DasGupta, A. Kaykas, R. T. Moon, N. Perrimon, Functional genomic analysis of the Wnt-wingless signaling pathway. *Science* **308**, 826–833 (2005).
19. G. H. Baeg, R. Zhou, N. Perrimon, Genome-wide RNAi analysis of JAK/STAT signaling components in *Drosophila*. *Genes Dev.* **19**, 1861–1870 (2005).
20. M. N. Krishnan, A. Ng, B. Sukumaran, F. D. Gilfoy, P. D. Uchil, H. Sultana, A. L. Brass, R. Adametz, M. Tsui, F. Qian, R. R. Montgomery, S. Lev, P. W. Mason, R. A. Koski, S. J. Elledge, R. J. Xavier, H. Agaisse, E. Fikrig, RNA interference screen for human genes associated with West Nile virus infection. *Nature* **455**, 242–245 (2008).
21. A. L. Brass, D. M. Dykxhoorn, Y. Benita, N. Yan, A. Engelman, R. J. Xavier, J. Lieberman, S. J. Elledge, Identification of host proteins required for HIV infection through a functional genomic screen. *Science* **319**, 921–926 (2008).
22. I. Derré, M. Pypaert, A. Dautry-Varsat, H. Agaisse, RNAi screen in *Drosophila* cells reveals the involvement of the Tom complex in *Chlamydia* infection. *PLoS Pathog.* **3**, 1446–1458 (2007).
23. C. A. Elwell, A. Ceesay, J. H. Kim, D. Kalman, J. N. Engel, RNA interference screen identifies Abl kinase and PDGFR signaling in *Chlamydia trachomatis* entry. *PLoS Pathog.* **4**, e1000021 (2008).
24. C. Rommel, G. Radziwill, J. Lovric, J. Noeldeke, T. Heinicke, D. Jones, A. Aitken, K. Moelling, Activated Ras displaces 14-3-3 protein from the amino terminus of c-Raf-1. *Oncogene* **12**, 609–619 (1996).
25. S. Zimmermann, K. Moelling, Phosphorylation and regulation of Raf by Akt (protein kinase B). *Science* **286**, 1741–1744 (1999).
26. J. Kuai, E. Nickbarg, J. Wooters, Y. Qiu, J. Wang, L. L. Lin, Endogenous association of TRAF2, TRAF3, cIAP1, and Smac with lymphotoxin β receptor reveals a novel mechanism of apoptosis. *J. Biol. Chem.* **278**, 14363–14369 (2003).
27. J. Papin, S. Subramaniam, Bioinformatics and cellular signaling. *Curr. Opin. Biotechnol.* **15**, 78–81 (2004).
28. E. M. Esparza, R. H. Arch, Glucocorticoid-induced TNF receptor, a costimulatory receptor on naive and activated T cells, uses TNF receptor-associated factor 2 in a novel fashion as an inhibitor of NF-κB activation. *J. Immunol.* **174**, 7875–7882 (2005).
29. A. M. Castellino, G. J. Parker, I. V. Boronenkov, R. A. Anderson, M. V. Chao, A novel interaction between the juxtamembrane region of the p55 tumor necrosis factor receptor and phosphatidylinositol-4-phosphate 5-kinase. *J. Biol. Chem.* **272**, 5861–5870 (1997).
30. S. Nagata, Apoptosis by death factor. *Cell* **88**, 355–365 (1997).
31. T. Yoneda, K. Imaizumi, K. Oono, D. Yui, F. Gomi, T. Katayama, M. Tohyama, Activation of caspase-12, an endoplastic reticulum (ER) resident caspase, through tumor necrosis factor receptor-associated factor 2-dependent mechanism in response to the ER stress. *J. Biol. Chem.* **276**, 13935–13940 (2001).
32. Y. H. Chang, S. L. Hsieh, M. C. Chen, W. W. Lin, Lymphotoxin β receptor induces interleukin 8 gene expression via NF-κB and AP-1 activation. *Exp. Cell Res.* **278**, 166–174 (2002).
33. J. M. Kyriakis, J. Avruch, Mammalian mitogen-activated protein kinase signal transduction pathways activated by stress and inflammation. *Physiol. Rev.* **81**, 807–869 (2001).
34. V. Adler, M. R. Pincus, P. W. Brandt-Rauf, Z. Ronai, Complexes of p21RAS with JUN N-terminal kinase and JUN proteins. *Proc. Natl. Acad. Sci. U.S.A.* **92**, 10585–10589 (1995).
35. C. M. Larsen, K. A. Wadt, L. F. Juhl, H. U. Andersen, A. E. Karlsen, M. S. Su, K. Seedorf, L. Shapiro, C. A. Dinarello, T. Mandrup-Poulsen, Interleukin-1β-induced rat pancreatic islet nitric oxide synthesis requires both the p38 and extracellular signal-regulated kinase 1/2 mitogen-activated protein kinases. *J. Biol. Chem.* **273**, 15294–15300 (1998).

36. K. Rajalingam, C. Wunder, V. Brinkmann, Y. Churin, M. Hekman, C. Sievers, U. R. Rapp, T. Rudel, Prohibitin is required for Ras-induced Raf-MEK-ERK activation and epithelial cell migration. *Nat. Cell Biol.* **7**, 837–843 (2005).
37. H. W. Wu, H. F. Li, X. Y. Wu, J. Zhao, J. Guo, Reactive oxygen species mediate ERK activation through different Raf-1-dependent signaling pathways following cerebral ischemia. *Neurosci. Lett.* **432**, 83–87 (2008).
38. M. A. Scidmore, T. Hackstadt, Mammalian 14-3-3β associates with the *Chlamydia trachomatis* inclusion membrane via its interaction with IncG. *Mol. Microbiol.* **39**, 1638–1650 (2001).
39. H. G. Chu, S. K. Weeks, D. M. Gilligan, D. D. Rockey, Host α-adducin is redistributed and localized to the inclusion membrane in *Chlamydia*- and *Chlamydophila*-infected cells. *Microbiology* **154**, 3848–3855 (2008).
40. N. Paland, L. Bohme, R. K. Gurumurthy, A. Maurer, A. J. Szczepek, T. Rudel, Reduced display of tumor necrosis factor receptor I at the host cell surface supports infection with *Chlamydia trachomatis*. *J. Biol. Chem.* **283**, 6438–6448 (2008).
41. F. Njau, U. Wittkop, M. Rohde, H. Haller, A. Klos, A. D. Wagner, In vitro neutralization of tumor necrosis factor-α during *Chlamydia pneumoniae* infection impairs dendritic cells maturation/function and increases chlamydial progeny. *FEMS Immunol. Med. Microbiol.* **55**, 215–225 (2009).
42. C. Du, M. Fang, Y. Li, L. Li, X. Wang, Smac, a mitochondrial protein that promotes cytochrome c-dependent caspase activation by eliminating IAP inhibition. *Cell* **102**, 33–42 (2000).
43. A. M. Verhagen, P. G. Ekert, M. Pakusch, J. Silke, L. M. Connolly, G. E. Reid, R. L. Moritz, R. J. Simpson, D. L. Vaux, Identification of DIABLO, a mammalian protein that promotes apoptosis by binding to and antagonizing IAP proteins. *Cell* **102**, 43–53 (2000).
44. K. Rajalingam, M. Sharma, N. Paland, R. Hurwitz, O. Thieck, M. Oswald, N. Machuy, T. Rudel, IAP-IAP complexes required for apoptosis resistance of *C. trachomatis*–infected cells. *PLoS Pathog.* **2**, e114 (2006).
45. A. Hindley, W. Kolch, Extracellular signal regulated kinase (ERK)/mitogen activated protein kinase (MAPK)-independent functions of Raf kinases. *J. Cell Sci.* **115**, 1575–1581 (2002).
46. N. Tapinos, A. Rambukkana, Insights into regulation of human Schwann cell proliferation by Erk1/2 via a MEK-independent and p56Lck-dependent pathway from leprosy bacilli. *Proc. Natl. Acad. Sci. U.S.A.* **102**, 9188–9193 (2005).
47. N. Machuy, B. Thiede, K. Rajalingam, C. Dimmler, O. Thieck, T. F. Meyer, T. Rudel, A global approach combining proteome analysis and phenotypic screening with RNA interference yields novel apoptosis regulators. *Mol. Cell. Proteomics* **4**, 44–55 (2005).
48. N. Malo, J. A. Hanley, S. Cerquozzi, J. Pelletier, R. Nadon, Statistical practice in high-throughput screening data analysis. *Nat. Biotechnol.* **24**, 167–175 (2006).
49. S. Falcon, R. Gentleman, Using GOstats to test gene lists for GO term association. *Bioinformatics* **23**, 257–258 (2007).
50. Acknowledgments: We thank C. Dimmler, D. Khalil, and J.-D. Manntz for technical support; E. Gonzalez for help during hit validation; and L. A. Ogilvie for editing the manuscript. We thank D. Heuer and H. Al-Younes for suggesting the positive and negative controls used in this assay. We also thank the *Chlamydia* group at the Max Planck Institute for Infection Biology for helpful comments on the manuscript.
Funding: This study was supported by the Bundesministerium für Forschung und Technologie through the ECIBUG project (grant 0313935C) and the RNAi-Net (grant 0313938A) to T.F.M. The funders had no role in study design, data collection and analysis, decision to publish, or preparation of the manuscript.
Author contributions: R.K.G., A.P.M., N.M., S.H., and T.F.M. conceived the project; R.K.G., A.P.M., N.M., S.H., and T.F.M. designed experiments; R.K.G. performed experiments; R.K.G. and S.H. established the automated microscopic readout; R.K.G., A.P.M., N.M., K.P.P., and J.S. conducted bioinformatics analysis; N.M., T.R., and T.F.M. established the screening platform; R.K.G., A.P.M., N.M., and T.F.M. wrote the manuscript.
Competing interests: The authors declare no competing interests.

Submitted 17 September 2009
Accepted 26 February 2010
Final Publication 16 March 2010
10.1126/scisignal.2000651
Citation: R. K. Gurumurthy, A. P. Mäurer, N. Machuy, S. Hess, K. P. Pleissner, J. Schuchhardt, T. Rudel, T. F. Meyer, A loss-of-function screen reveals Ras- and Raf-independent MEK-ERK signaling during *Chlamydia trachomatis* infection. *Sci. Signal.* **3**, ra21 (2010).

Science Signaling

A Loss-of-Function Screen Reveals Ras- and Raf-Independent MEK-ERK Signaling During *Chlamydia trachomatis* Infection

Rajendra Kumar Gurumurthy, André P. Mäurer, Nikolaus Machuy, Simone Hess, Klaus P. Pleissner, Johannes Schuchhardt, Thomas Rudel and Thomas F. Meyer

Sci. Signal. **3** (113), ra21.
DOI: 10.1126/scisignal.2000651

Decoupling a MAPK Pathway

Chlamydia trachomatis (*Ctr*) is an obligate, intracellular bacterial pathogen that causes a number of sexually transmitted diseases and the infectious eye disease, trachoma. *Ctr* cycles between an extracellular, infectious state known as the elementary body and an intracellular, metabolically active and replicating state known as the reticulate body. *Ctr* reticulate bodies accumulate within the inclusion, a membrane-bound vacuole. Gurumurthy *et al*. performed an RNA interference (RNAi) –based screen of infected epithelial cells and identified 59 factors that regulated *Ctr* infectivity. Knockdown of two of these, K-Ras and Raf-1, resulted in the increased growth of *Ctr*. Infection by *Ctr* led to the phosphorylation and inactivation of Raf-1 and its recruitment to the inclusion rather than to the plasma membrane where it normally triggers the MEK-ERK pathway, which is important for cell survival. Despite the inactivation of Raf-1, ERK activation was normal in infected cells, ensuring survival of the cells and growth of the pathogen. Thus, *Ctr* differentially modulates components of the Ras-ERK pathway to its own advantage.